

Engineering quantum Mpemba effect by Liouvillian skin effect

Xiang Zhang,¹ Chen Sun,¹ and Fuxiang Li^{1,*}

¹*School of Physics and Electronics, Hunan University, Changsha 410082, China*

(Dated: January 23, 2026)

We propose a new approach to engineer the quantum Mpemba effect (QME)—wherein an initial state farther from system relaxes faster than a close one—by the Liouvillian skin effect (LSE) in open quantum systems. Moreover, the LSE serves as an ideal platform for realizing the QME and the spatial profile of the LSE provides a straightforward pathway for the initial state preparation, thereby enabling readily accessible experimental preparation. Focusing on the quadratic Lindbladians, we consider two concrete cases to design the initial states, thereby realizing the QME. Interestingly, we uncover a new kind of QME (QME-III) that is distinct from the two typical scenarios, manifested as two reversals in the Hilbert-Schmidt distance at two different times. In particular, the LSE provides a physically more intuitive understanding of the QME.

Introduction.— The relaxation process in open quantum systems holds fundamental significance across both nonequilibrium physics and applied quantum technologies. Effectively steering the relaxation process could accelerate quantum computation[1–3], enable the development of faster search algorithms [4–6], and facilitate the preparation of quantum states essential for quantum-enhanced metrology [7, 8]. Among the various strategies for accelerating relaxation toward thermal equilibrium, a particularly intriguing approach is inspired by the so-called Mpemba effect, a counterintuitive relaxation anomaly in which a hotter system can cool faster than a colder one [9, 10]. This phenomenon was first understood in the context of classical nonequilibrium physics [11–13], and then extended to quantum systems, in both open system [14–21] and closed systems [22–24].

When searching for the optimal initial state to accelerate relaxation, the existing implementations based on quantum Mpemba effect (QME) typically require careful initial-state design and fine-tuning of control parameters [25, 26], or alternatively, rely on temporarily coupling the system to a reset channel [20]. In this Letter, by uncovering the deep relation between Mpemba effect and Liouvillian skin effect, we propose a straightforward and intuitive approach for selecting the initial states and realizing the Mpemba effect in open quantum systems. The skin effect is a distinctive phenomenon in non-hermitian systems, which refers to the exponential localization of a vast majority of eigenstates near the boundaries. The non-Hermitian skin effect fundamentally alters the conventional bulk-boundary correspondence, and yields novel phenomena in wavefunction dynamics such as unidirectional amplification and quantum sensing enhancement. More recently, the skin effect was identified to exist in the Liouvillian superoperator due to its intrinsic non-Hermiticity and was dubbed the Liouvillian skin effect (LSE) [27–33]. It has also been pointed out that the Liouvillian skin effect has a striking influence on the relaxation processes [27, 34–38]. However, the re-

lation between LSE and QME has not been explored.

In this Letter, we explore the spatial structure of relaxation process in open quantum system and illustrate that Liouvillian skin effect enables a straightforward and intuitive approach for selecting the initial states and realizing the Mpemba effect in open quantum systems. The initial state can be prepared simply by exploiting the spatial distribution of the particle numbers induced by the Liouvillian skin effect. This approach circumvents the necessity to construct a specific unitary transformation for the initial state or the requirement that the initial state must be pure state, or the strict constraints, such as assuming pure initial states or requiring the second-largest eigenvalue of the Lindbladian to be real. Our work provides a more intuitive physical picture to understand the underlying mechanism of quantum Mpemba effect and opens the avenue for the study of interplay between relaxation process and Liouvillian Hamiltonian?

We shall restrict our attention to Markovian open quantum system with size L described by a Hilbert space \mathcal{H} of finite dimension 2^L such that the time evolution of the reduced density matrix of the system, ρ , is described by the Lindblad master equation:

$$\frac{d\rho}{dt} = -i[H, \rho] + \sum_{\mu} (2L_{\mu}\rho L_{\mu}^{\dagger} - \{L_{\mu}^{\dagger}L_{\mu}, \rho\}), \quad (1)$$

where H is the Hamiltonian of the system describing the unitary evolution, and L_{μ} 's are the jump operators describing the incoherent dynamics induced by the coupling to the environment. The right-hand side of Eq. (1) defines the Liouvillian superoperator $\hat{\mathcal{L}}$ (also called Lindbladian), acting on a doubled Hilbert space $\mathcal{H} \otimes \mathcal{H}^*$, and the master equation is conveniently written as $\partial_t |\rho\rangle\rangle = \hat{\mathcal{L}}|\rho\rangle\rangle$, where $|\rho\rangle\rangle$ now refers to the vectorized version of the reduced density matrix of dimension $2^L \times 2^L$ by flattening $|v_1\rangle\langle v_2|$ into $|v_1\rangle\otimes|v_2\rangle$ and the inner product in this linear space is defined as $\langle\langle A|B\rangle\rangle = \text{tr}(A^{\dagger}B)$.

Formally, we can write down the general evolution of an initial density matrix $\rho(t)$ as

$$|\rho(t)\rangle\rangle = e^{\mathcal{L}t}|\rho_0\rangle\rangle = |\rho_{ss}\rangle\rangle + \sum_{i=2}^{2^L} e^{\epsilon_i t} \langle\langle l_i|\rho_0\rangle\rangle |r_i\rangle\rangle, \quad (2)$$

* Corresponding author: fuxiangli@hnu.edu.cn

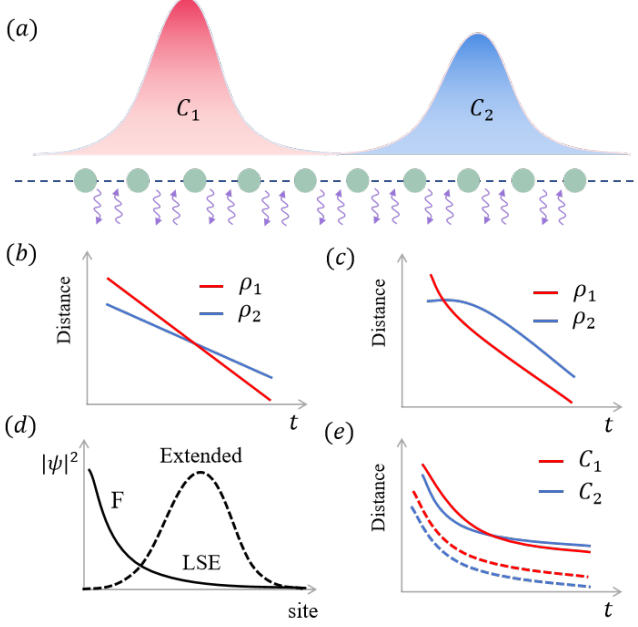


FIG. 1. Schematic illustration of the quantum Mpemba effect (QME) engineered by the Liouvillian skin effect (LSE). (a) Sketch of the model and the selection of the initial states C_1 and C_2 according to the spatial profile of density of particle numbers, corresponding to the more and less particles. The purple arrows represent the linear gain and loss operators $L_j^{g/l}$ at site j . (b) and (c) are the two typical QME (QME-I and QME-II). For (b), QME-I is realized when one unitary transforms the initial state ρ_2 to another state ρ_1 which makes the coefficient of the slowest mode disappear so that $\rho_1(t) - \rho_{ss} \propto \exp(t\text{Re}\epsilon_3)$. For (c), QME-II can occur at early times even though asymptotic decay rates remain unchanged if $|a_2^c| > |a_2^f|$, where the coefficients $a_2^{c(f)}$ denote the overlaps between the initial state and the slowest modes for close (farther) states, as shown in Fig. 1 (c), which has an analogy in classical Mpemba effect [11].

In this work, we propose an entirely novel approach to observe QME through the Liouvillian skin effect in quadratic Lindbladians. The advantages are as follows:

(I). *It completely circumvents the need to construct a specific unitary transformation.*

(II). *The initial state is prepared simply by exploiting the spatial distribution of the particle numbers induced by the Liouvillian skin effect.*

(III). *It provides a more intuitive physical picture to understand the underlying mechanism of QME.*

(IV). *We uncover a new kind of QME (QME-III) that is different from QME-I and QME-II when the correlation between different lattice sites is introduced.*

Below we will discuss open quantum systems governed by a general class of Lindblad master equations to illustrate our idea, namely, the case of a Markovian bath with linear jump operators [34, 41–46]. In the main text, we only consider fermionic system, the bosonic system is discussed in SM. In this regime, the Lindblad master equation is quadratic and these “quadratic Lindbladians” can be captured by a non-Hermitian single-particle matrix which describes internal dynamics as well as system-environment coupling.

Quadratic Lindbladians.— We briefly review the third quantization approach [41–44] that essentially amounts to flattening the density matrix in a way that naturally respects fermion statistics. For our purposes, the main result we need is that the superoperator $\hat{\mathcal{L}}$ can be brought into the diagonal form

$$\hat{\mathcal{L}} = \sum_{i=1}^{2L} \beta_i \hat{b}_i' \hat{b}_i, \quad \beta_i \in \mathbb{C}, \quad \text{Re}\beta_i < 0, \quad (3)$$

where the operators \hat{b}_i' , \hat{b}_i are called the normal master modes that almost satisfy canonical anticommutation relations $\{\hat{b}_i, \hat{b}_j\} = \{\hat{b}_i', \hat{b}_j'\} = 0$, $\{\hat{b}_i, \hat{b}_j'\} = \delta_{i,j}$ and the eigenvalues β_i are known as rapidities. The nonequilibrium steady state, corresponding to vacuum: $\hat{b}_i |\rho_{ss}\rangle = 0$. The “excitations” are the relaxation modes $\hat{b}_i \hat{b}_j' |\rho_{ss}\rangle = 0$ that decay toward the steady state with a rate $e^{(\beta_i + \beta_j)t}$. Here, we use two \hat{b}' operators instead of one, because physical density matrices have even fermion

where $|\rho_{ss}\rangle$ is the unique steady state that is the right eigenoperator of the Liouvillian superoperator \mathcal{L} associated with the zero eigenvalue. $|r_i\rangle$ and $|l_i\rangle$ are the left and right eigenvectors corresponding to the eigenvalue λ_i which satisfy $\hat{\mathcal{L}}|r_i\rangle = \epsilon_i|r_i\rangle$ and $\hat{\mathcal{L}}^\dagger|l_i\rangle = \epsilon_i^*|l_i\rangle$. The right and left eigenmodes corresponding to different eigenvalues are orthogonal to each other: $\langle\langle l_i | r_j \rangle\rangle = 0$. Suppose that all eigenvalues are arranged in descending order of their real parts: $0 = \text{Re}\epsilon_1 > \text{Re}\epsilon_2 \geq \text{Re}\epsilon_3 \geq \dots$, the spectral gap is $|\text{Re}\epsilon_2|$ and defines the longest timescale in the system such that $\rho(t) - \rho_{ss} \propto \exp(t\text{Re}\epsilon_2)$.

In Ref. [14], the authors show that an exponential speed up to the steady state can be achieved by a unitary transform of the initial state to another state

parity. In SM, we show that both the “single-particle” eigenvalues β_i of \hat{L} , as well as creation operators \hat{b}'_i (but not the \hat{b}_i), are fully determined by the spectrum and eigenvectors of the effective non-Hermitian Hamiltonian

$$\mathcal{H}_{\text{eff}} = iH^T - (M_l^T + M_g). \quad (4)$$

In particular, the eigenvalues of \mathcal{H}_{eff} with size L are denoted by λ_i , then the β_i are given by

$$\begin{aligned} \beta_i &= \lambda_i, & i &= 1, 2, \dots, L, \\ \beta_i &= -\lambda_{i-L}^*, & i &= N+1, \dots, 2L. \end{aligned} \quad (5)$$

The real space profile of the creation operators \hat{b}'_i is exactly the same as that of the eigenvectors of \mathcal{H}_{eff} . Another way to see that \mathcal{H}_{eff} governs the relaxation dynamics is the time evolution equation of the correlation matrix $C_{ij}(t) = \text{Tr}[c_i^\dagger c_j \rho]$ [34, 36]:

$$\frac{dC(t)}{dt} = \mathcal{H}_{\text{eff}} C(t) + C(t) \mathcal{H}_{\text{eff}}^\dagger + 2M_g. \quad (6)$$

The steady state correlation C_{ss} , to which long time evolution of any initial state converges, is determined by $dC_{ss}/dt = 0$, or the Lyapunov equation $\mathcal{H}_{\text{eff}} C_{ss} + C_{ss} \mathcal{H}_{\text{eff}}^\dagger + 2M_g = 0$. Meanwhile, the effective non-Hermitian Hamiltonian \mathcal{H}_{eff} can be decoupled as $\mathcal{H}_{\text{eff}} = \sum_i \lambda_i |R^i\rangle\langle L^i|$ [47]. Here, λ_i is the i -th eigenvalues and R^i (L^i) the corresponding right (left) eigenvectors. Then the steady state C_{ss} can be written as:

$$C_{ss} = \sum_{i,j} -\frac{|R^i\rangle\langle L^i|2M_g|L^j\rangle\langle R^j|}{\lambda_i + \lambda_j^*}. \quad (7)$$

Introducing the deviation $\delta C(t) = C(t) - C_{ss}$, the evolution becomes $d\delta C(t)/dt = \mathcal{H}_{\text{eff}} \delta C(t) + \delta C(t) \mathcal{H}_{\text{eff}}^\dagger$. The solution to this equation is

$$\delta C(t) = e^{\mathcal{H}_{\text{eff}} t} \delta C_0 e^{\mathcal{H}_{\text{eff}}^\dagger t}. \quad (8)$$

In terms of eigenvalue and eigenstate of \mathcal{H}_{eff} , Eq. (8) can also be written as:

$$\delta C(t) = \sum_{i,j} e^{(\lambda_i + \lambda_j^*)t} |R^i\rangle\langle L^i| \delta C_0 |L^j\rangle\langle R^j|. \quad (9)$$

From this equation, the relaxation behavior of open quantum system should be dominated by the real part of the eigenvalues. However, if the system possesses skin effect, then there emerges extra relaxation channel. Moreover, if the right-eigenstates R^i are localized on the left side of the one-dimensional system, then the L^i would be localized on the right end. Therefore, one can easily tune the relaxation process by choosing different initial conditions for δC_0 which lead to drastically different values of the term $\langle L^i | \delta C_0 | L^j \rangle$, and thus achieve the goals of quantum Mpemba effect.

Quantum Mpemba effect.— There are many quantities that may be used as metrics for measuring the distance

between two states [25]. In this work, we focus on Frobenius or Hilbert-Schmidt distance [48, 49] to quantify the distance from the steady state. The Hilbert-Schmidt distance is one of the prominent distance measures in quantum information theory which plays a crucial role in diverse problems, such as construction of entanglement witnesses [50, 51], quantum algorithms in machine learning [52], and quantum-state tomography [53, 54]. The Hilbert-Schmidt distance is defined as

$$\mathcal{D}_{HS}(C(t), C_{ss}) = \sqrt{\text{Tr}[(C(t) - C_{ss})^2]}. \quad (10)$$

Mathematically, the Hilbert-Schmidt distance can be understood as the Euclidean distance between two vectorized matrices. The Hilbert-Schmidt distance has also been used to observe the strong quantum Mpemba effect in Markovian systems [14]. In open quantum systems with linear particle gain and loss operators, this metric of distance is monotonic in time, thus allowing one to observe the quantum Mpemba effects. The QME occurs if there exists a time t_M such that the Hilbert-Schmidt distance is reversed, $\mathcal{D}_{HS}^1 > \mathcal{D}_{HS}^2$ for $t > t_M$, where the distance between two initial states satisfy $\mathcal{D}_{HS}^1 < \mathcal{D}_{HS}^2$ for $t = 0$.

We now consider a prototypical model which can be either fermionic or bosonic under open boundary conditions, as shown in Fig. 1. The corresponding Hamiltonian is given by

$$H = -J \sum_{j=1}^L (c_j^\dagger c_{j+1} + c_{j+1}^\dagger c_j). \quad (11)$$

Here, L is the system size. Specifically, gain and loss jump operators are labeled by purple arrows in Fig. 1 and take the form of (Type-I) [55, 56]

$$\begin{aligned} L_j^g &= \sqrt{\frac{\gamma_g}{2}} (c_j^\dagger + i c_{j+1}^\dagger) \\ L_j^l &= \sqrt{\frac{\gamma_l}{2}} (c_j - i c_{j+1}), \end{aligned} \quad (12)$$

where $\gamma_{l/g}$ is the dissipation rate, and j labels the position of lattice site. These jump operators can be realized within the framework of reservoir engineering [57–59].

From Eq. (4), the effective non-Hermitian Hamiltonian \mathcal{H}_{eff} in real space is

$$\mathcal{H}_{\text{eff}} = -iH_{HN} - \sum_{j=1}^L 2\Gamma c_j^\dagger c_j \quad (13)$$

with

$$H_{HN} = \sum_{j=1}^L \left((J + \Gamma) c_j^\dagger c_{j+1} + (J - \Gamma) c_{j+1}^\dagger c_j \right) \quad (14)$$

where $\Gamma = (\gamma_l + \gamma_g)/2$, and H_{HN} is the Hamiltonian for the Hatano-Nelson model [60–62]. The eigenvalues of effective Hamiltonian \mathcal{H}_{eff} under open boundary conditions

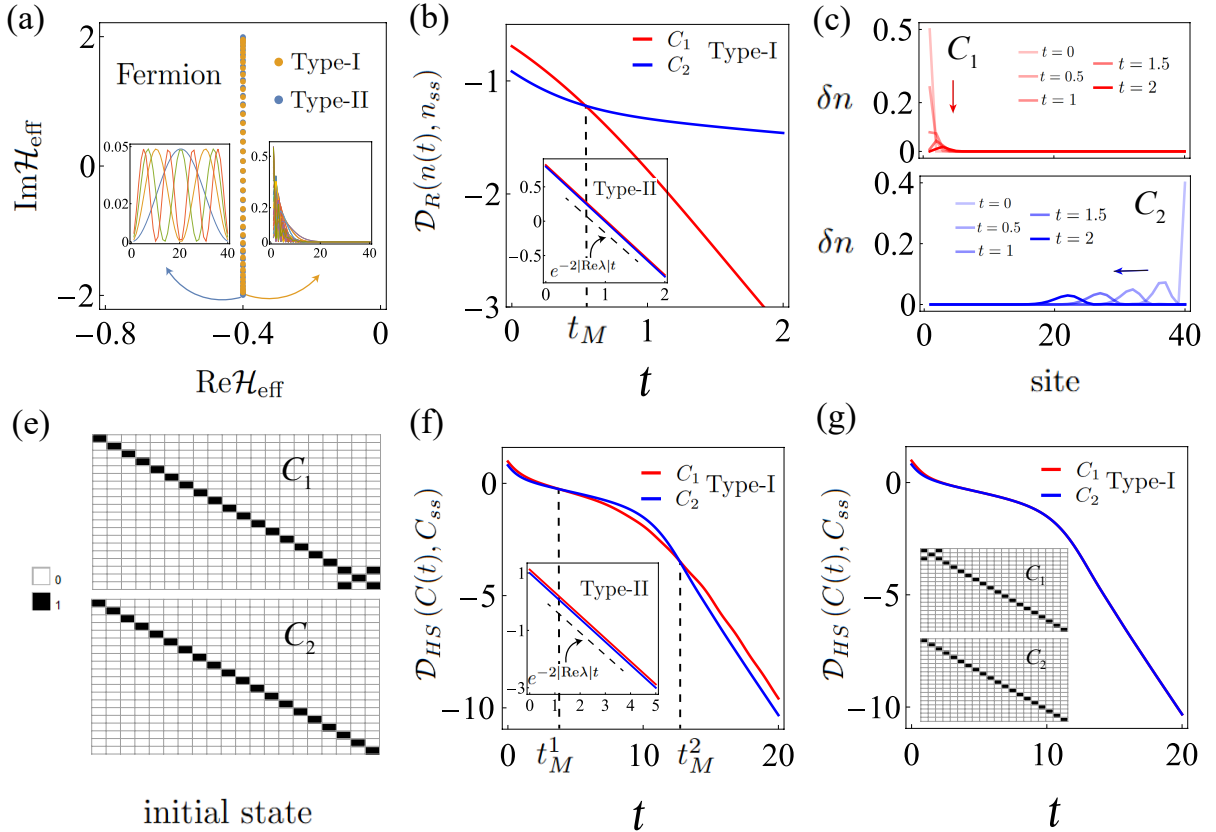


FIG. 2. Quantum Mpemba effects in quadratic fermionic Lindbladians for *Case-I* ((b)-(c)) and *Case-II* ((e)-(g)), corresponding to the QME-II and QME-III. (a) The eigenvalues (Eq. (15)) of the effective Hamiltonian \mathcal{H}_{eff} for Type-I (yellow) and Type-II (blue) gain and loss jump operators. Parameters are $J = 1$, $\gamma_g = \gamma_l = 0.2$ and $L = 40$. The corresponding eigenstates of Type-I and Type-II jump operators are shown in the inset. (b) The reduced distance $\mathcal{D}_R(n(t), n_{ss}) = \sqrt{\sum_j^L (n^j(t) - n_{ss}^j)^2}$ varies as a function of time for two initial states C_1 and C_2 . For Type-I jump operators, the initial state C_1 farther from the steady state relaxes faster than a close one C_2 at early times, the so-called QME. The inset is for Type-II jump operators. (c) The deviation of density of particle numbers δn vary as a function lattice site at different times for the two initial states C_1 and C_2 . (e) The two initial states C_1 and C_2 . The diagonal elements of both states are 1. In addition, initial state C_1 also has off-diagonal elements at the right edge (the opposite direction of LSE). Parameters are $J = 1$, $\gamma_g = \gamma_l = 0.2$ and $L = 20$. (f) The Hilbert-Schmidt distance $\mathcal{D}_{HS}(C(t), C_{ss}) = \sqrt{\text{Tr}[(C(t) - C_{ss})^2]}$ changes as a function of time. For Type-I jump operators, the two typical QME in Figs. 1(b) and (c) can occur. The inset is for Type-II jump operators. (g) The off-diagonal elements of initial state C_1 reside in the left edge (the direction of LSE) so that there is no QME for Type-I jump operators.

are given by

$$\lambda_k = -2\Gamma \pm i2\sqrt{(J + \Gamma)(J - \Gamma)} \cos k, \quad (15)$$

where the values of momentum k are $2\pi m/(L + 1)$ with $m = 0, \dots, L - 1$. From Eq. (13), the strength of left hopping is greater than right hopping, thus manifested as a leftward Liouvillian skin effect, as demonstrated in inset of Fig. 2 (a). For comparison, we also examine an alternative form of gain and loss jump operators (Type-II) : $L_j^g = \sqrt{\gamma_g/2}(c_j^\dagger + c_{j+1}^\dagger)$ and $L_j^l = \sqrt{\gamma_l/2}(c_j - c_{j+1})$, enabling that the effective non-Hermitian Hamiltonian \mathcal{H}_{eff} has no Liouvillian skin effect.

We present the energy spectrum of the effective Hamiltonian \mathcal{H}_{eff} in Fig. 2 (a) with Type-I and Type-II jump operators. Interestingly, the energy spectrum of Type-I

nearly overlaps with the spectrum of Type-II and the real part of energy remains unchanged. Globally, the stability of quadratic Lindbladians can be quantified with the Liouvillian gap $\Delta = \text{Re}\lambda_k$. The Liouvillian gap Δ is always negative and there always exist a steady state. For this fermionic system, we consider a uniform dissipation rate for loss and gain operator and set $\gamma_l = \gamma_g$. Under this parameter setting, the steady state Eq. (7) is $C_{ss} = (1/2)I_{N \times N}$ [34].

We now demonstrate that the LSE provides a natural platform for realizing the QME. In particular, we consider two distinct cases to construct reasonable initial states, built on the LSE, to engineer the QME-II and QME-III.

Case-I.— First, we consider a simple case that the initial correlation C solely comprises diagonal matrix ele-

ments, indicating vanishing inter-site correlations. In this setting, the Hilbert-Schmidt distance (Eq. (10)) amounts to measuring the relaxation behavior of the time-dependent fermion particle number toward its steady state value n_{ss} . The corresponding reduced distance from the steady state is $\mathcal{D}_R(n(t), n_{ss}) = \sqrt{\sum_j^L (n^j(t) - n_{ss}^j)^2}$ with $n^j = C_{j,j}$ being the particle numbers at site j . In SM, we also directly exploit the trace distance to characterize the distance between two density matrix for a finite chain of size $L = 5$ via exact diagonalization.

In particular, we choose two different initial states C_1 and C_2 ruled in Fig. 1, corresponding to the many particles and the few particles, labeled by red and blue regions. The deviation from steady state of the two initial states is chosen as $\delta C_{1,11} = 0.5$ and $\delta C_{2,LL} = 0.4$, i.e., the particle is initially localized on the left end or right end. Obviously, the initial distance \mathcal{D}_R^1 is larger than \mathcal{D}_R^2 at time $t = 0$. In Fig. 2 (b), for Type-I jump operators, the initial state C_1 farther from the steady state relaxes faster than a close one C_2 , so-called quantum Mpemba effect (QME-II). At time $t < t_M$, the distance $\mathcal{D}_R^1 > \mathcal{D}_R^2$, whereas, $\mathcal{D}_R^1 < \mathcal{D}_R^2$ for $t > t_M$. In stark contrast for Type-II jump operators where the eigenstates of the effective Hamiltonian \mathcal{H}_{eff} are extended, the initial state C_1 relaxes faster than C_2 at all times with the same decay exponent $2\text{Re}\lambda_k$, as demonstrated in inset of Fig. 2 (b).

In Fig. 2 (c), we plot the deviation of the particle number density $\delta n^j = n^j(t) - n_{ss}^j$ of each site at different times for initial state C_1 (top panel) and C_2 (bottom panel). The time evolution of particle number density displays different relaxation behaviors due to the LSE. For initial state C_2 that localizes at right edge, the particle propagates to the left with an increasing amplitude due to the non-Hermitian Hamiltonian H_{HN} with asymmetric hopping and at the same time decays exponentially with uniform rate 2Γ , according to Eq. (13). Altogether, the non-Hermitian amplification compensates the exponential decay and the particle decay follows instead a power-law damping, as discussed in Ref. [34]. For state C_1 with initial localization on the left edge, the particle propagates to right and at the same time decays exponentially with rate 2Γ . The total damping rate, however, is not simply 2Γ but larger than 2Γ since in the process of propagation to right, the particle also experiences a damping due to the non-Hermitian Hamiltonian with asymmetric hopping. The two distinctive relaxation processes for the states initially localized on the left and right edges enable the emergence of the QME, which is rooted in LSE.

Here we estimate the additional exponential decay rate (except the overall rate $4\Gamma t$) when the initial state sits at the leftmost site. When hopping to the right by one site, the asymmetric hopping strength produces a decaying factor $r = \sqrt{(J - \Gamma)/(J + \Gamma)}$ to the wavefunction, and hence a factor r^2 in its contribution to $\delta C(t)$. Hence, rightward propagation leads to the additional decay—suppose that at time t the state trav-

els a distance x to the right, then the decaying factor is r^{2x} . We take the propagation distance to be that of the $k = \pi/2$ mode which travels at the highest speed $\max(v_k) = 2\sqrt{(J + \Gamma)(J - \Gamma)}$. Then the decaying factor is $r^{2\max(v_k)t} = e^{2\log r \max(v_k)t}$. From this, the decay rate is estimated to be $2\log r \max|v_k| = 2\sqrt{(J + \Gamma)(J - \Gamma)\log[(J - \Gamma)/(J + \Gamma)]}$.

We have known that the underlying physical mechanism of the QME-II in our first case is rooted in the LSE. In addition, we can further mathematically explain the origin of QME-II based on Eq. (9). The term $\langle L^i | \delta C_0 | L^j \rangle$ exhibits a qualitatively distinct behavior for Type-I and Type-II jump operators. For Type-II, the eigenstates are extended. This results in nearly identical overlaps between the initial states C_1 and C_2 and the left eigenstates, leading to a pure exponential decay which is solely determined by the Liouvillian gap Δ . In stark contrast, when LSE is introduced in Type-I jump operators, the right eigenstates become exponentially localized at the left boundary [63]. And their corresponding left eigenstates are localized at the right boundary which leads to a significant discrepancy in overlaps $\langle L^i | \delta C_F^0 | L^j \rangle$, resulting in a significant different relaxation at early times for the two initial states C_1 and C_2 . The long time evolutions of both initial states are consistent with Ref. [34] which have the same asymptotic decay rates.

Case-II.— Next, we will consider a more complex but interesting case, involved with the relaxation of off-diagonal matrix elements in the initial state, namely, the relaxation of the correlation between different lattice site. Both initial states C_1 and C_2 are shown in Fig. 2 (e). The diagonal elements of C_1 and C_2 are same, $[1, 1, 1, \dots, 1]$. The first initial state C_1 consists not only of diagonal elements, but also of non-diagonal elements that reside in the right edge (the opposite direction of LSE). According to the Hilbert-Schmidt distance (Eq. (10)), the distance \mathcal{D}_{HS}^1 for initial state C_1 is larger than \mathcal{D}_{HS}^2 for initial state C_2 at time $t = 0$.

In Fig. (2)(f), for Type-I jump operators, we uncover a new kind of QME that is distinct from the two typical QME in Figs. 1 (b) and (c), characterized by two reversals in the Hilbert-Schmidt distance of the initial states C_1 and C_2 at two different times, dubbed as QME-III. At the early times, $t < t_M^1$, the Hilbert-Schmidt distance $\mathcal{D}_{HS}^1 > \mathcal{D}_{HS}^2$, whereas, $\mathcal{D}_{HS}^1 < \mathcal{D}_{HS}^2$ for $t > t_M^1$. As the time continues to evolve, QME occur again due to the different asymptotic decay rates, manifested as the Hilbert-Schmidt distance $\mathcal{D}_{HS}^1 < \mathcal{D}_{HS}^2$ at the long times $t_M^1 < t < t_M^2$, whereas, $\mathcal{D}_{HS}^1 > \mathcal{D}_{HS}^2$ for $t > t_M^2$. For Type-II jump operators, the inset exhibits no QME, manifested as the same decay behavior at all times. For comparison, we consider another case that the off-diagonal elements of the initial state C_1 reside in the left edge (the direction of LSE) and the second initial state C_2 remain unchanged. As shown in Fig. (2)(g), there is no QME to occur under this choose of initial states. The time evolution of the Hilbert-Schmidt distance of both initial states overlaps nearly with each other.

Conclusion.—In this work, we propose a new approach to observe the QME (where an initial state farther from system relaxes faster to the final equilibrium state than a close one) through the LSE in open quantum systems. In this regime, the LSE serves as an ideal platform for realizing the QME and the spatial profile of the LSE provides a straightforward pathway to select the initial state, thereby enabling readily accessible experimental preparation. We focus on a general class of Lindblad master equation with linear jump operators, the so-called quadratic Lindbladians. Under the third quantization, the property of the superoperator $\hat{\mathcal{L}}$ is fully determined by the effective non-Hermitian Hamiltonian \mathcal{H}_{eff} and the relaxation dynamics is monitored by the single-particle correlation C . According to the LSE, we consider two cases to engineer the QME. For *Case-I*, both initial states only contain diagonal elements and we design skillfully the two initial states to realize QME. For *Case-II*, built on the direction of LSE, the off-diagonal elements are

introduced to generate QME-III, manifested as two reversals in the Hilbert-Schmidt distance at two different times.

It should be noted that the mathematical structure underlying the QME-II in *Case-I* has an analogy [11] in classical Mpemba effect and can be seen as a quantum version of the classical Mpemba effect. In Ref. [11], the classical Mpemba effect is said to occur if $|a_2^c| > |a_2^h|$, where the coefficients $a_2^{(h)}$ denote the overlaps between the initial state and the slowest modes for cold (hot) states. However, there are some differences as follows: Firstly, our system is an open quantum system and the real parts of all eigenvalues of system are same. Secondly, the initial states can be constructed simply by exploiting the spatial distribution of the particle numbers induced by the LSE.

Note: In the preparation of the manuscript, we noticed that Ref. [64] appeared that has some overlap with our work.

[1] C. L. Degen, F. Reinhard, and P. Cappellaro, Quantum sensing, *Rev. Mod. Phys.* **89**, 035002 (2017).

[2] V. Giovannetti, S. Lloyd, and L. Maccone, Quantum-enhanced measurements: beating the standard quantum limit, *Science* **306**, 1330 (2004).

[3] S. Pirandola, B. R. Bardhan, T. Gehring, C. Weedbrook, and S. Lloyd, Advances in photonic quantum sensing, *Nat. Photonics* **12**, 724 (2018).

[4] F. Verstraete, M. M. Wolf, and J. I. Cirac, Quantum computation and quantum-state engineering driven by dissipation, *Nat. Phys.* **5**, 633 (2009).

[5] J. I. Cirac and P. Zoller, Goals and opportunities in quantum simulation, *Nat. Phys.* **8**, 264 (2012).

[6] S. Lloyd, Universal quantum simulators, *Science* **273**, 1073 (1996).

[7] S.-J. Wei, D. Ruan, and G.-L. Long, Duality quantum algorithm efficiently simulates open quantum systems, *Sci. Rep.* **6**, 30727 (2016).

[8] D. S. Wild, S. Gopalakrishnan, M. Knap, N. Y. Yao, and M. D. Lukin, Adiabatic quantum search in open systems, *Phys. Rev. Lett.* **117**, 150501 (2016).

[9] E. B. Mpemba and D. G. Osborne, Cool?, *Physics Education* **4**, 172 (1969).

[10] G. S. Kell, The freezing of hot and cold water, *American Journal of Physics* **37**, 564 (1969).

[11] Z. Lu and O. Raz, Nonequilibrium thermodynamics of the markovian mpemba effect and its inverse, *Proceedings of the National Academy of Sciences* **114**, 5083 (2017).

[12] I. Klich, O. Raz, O. Hirschberg, and M. Vucelja, Mpemba index and anomalous relaxation, *Phys. Rev. X* **9**, 021060 (2019).

[13] T. Van Vu and H. Hayakawa, Thermomajorization mpemba effect, *Phys. Rev. Lett.* **134**, 107101 (2025).

[14] F. Carollo, A. Lasanta, and I. Lesanovsky, Exponentially accelerated approach to stationarity in markovian open quantum systems through the mpemba effect, *Phys. Rev. Lett.* **127**, 060401 (2021).

[15] A. K. Chatterjee, S. Takada, and H. Hayakawa, Quantum mpemba effect in a quantum dot with reservoirs, *Phys. Rev. Lett.* **131**, 080402 (2023).

[16] A. Nava and R. Egger, Mpemba effects in open nonequilibrium quantum systems, *Phys. Rev. Lett.* **133**, 136302 (2024).

[17] A. Nava and R. Egger, Pontus-mpemba effects, *Phys. Rev. Lett.* **135**, 140404 (2025).

[18] M. Moroder, O. Culhane, K. Zawadzki, and J. Goold, Thermodynamics of the quantum mpemba effect, *Phys. Rev. Lett.* **133**, 140404 (2024).

[19] I. Medina, O. Culhane, F. C. Binder, G. T. Landi, and J. Goold, Anomalous discharging of quantum batteries: The ergotropic mpemba effect, *Phys. Rev. Lett.* **134**, 220402 (2025).

[20] R. Bao and Z. Hou, Accelerating quantum relaxation via temporary reset: A mpemba-inspired approach, *Phys. Rev. Lett.* **135**, 150403 (2025).

[21] S. Kochsiek, F. Carollo, and I. Lesanovsky, Accelerating the approach of dissipative quantum spin systems towards stationarity through global spin rotations, *Phys. Rev. A* **106**, 012207 (2022).

[22] F. Ares, S. Murciano, and P. Calabrese, Entanglement asymmetry as a probe of symmetry breaking, *Nature Communications* **14**, 2036 (2023).

[23] S. Liu, H.-K. Zhang, S. Yin, and S.-X. Zhang, Symmetry restoration and quantum mpemba effect in symmetric random circuits, *Phys. Rev. Lett.* **133**, 140405 (2024).

[24] H. Yu, S. Liu, and S.-X. Zhang, Quantum mpemba effects from symmetry perspectives, *AAPPS Bulletin* **35**, 17 (2025).

[25] F. Ares, P. Calabrese, and S. Murciano, The quantum mpemba effects, *Nature Reviews Physics* **1** (2025).

[26] G. Teza, J. Bechhoefer, A. Lasanta, O. Raz, and M. Vucelja, Speedups in nonequilibrium thermal relaxation: Mpemba and related effects, arXiv preprint (2025), [arXiv:2502.01758 \[cond-mat.stat-mech\]](https://arxiv.org/abs/2502.01758).

[27] T. Haga, M. Nakagawa, R. Hamazaki, and M. Ueda,

Liouvillian skin effect: Slowing down of relaxation processes without gap closing, *Phys. Rev. Lett.* **127**, 070402 (2021).

[28] S. E. Begg and R. Hanai, Quantum criticality in open quantum spin chains with nonreciprocity, *Phys. Rev. Lett.* **132**, 120401 (2024).

[29] L. Mao, X. Yang, M.-J. Tao, H. Hu, and L. Pan, Liouvillian skin effect in a one-dimensional open many-body quantum system with generalized boundary conditions, *Phys. Rev. B* **110**, 045440 (2024).

[30] F. Yang, Q.-D. Jiang, and E. J. Bergholtz, Liouvillian skin effect in an exactly solvable model, *Phys. Rev. Res.* **4**, 023160 (2022).

[31] S. Hamanaka, K. Yamamoto, and T. Yoshida, Interaction-induced liouvillian skin effect in a fermionic chain with a two-body loss, *Phys. Rev. B* **108**, 155114 (2023).

[32] Z. Wang, Y. Lu, Y. Peng, R. Qi, Y. Wang, and J. Jie, Accelerating relaxation dynamics in open quantum systems with liouvillian skin effect, *Phys. Rev. B* **108**, 054313 (2023).

[33] D.-H. Cai, W. Yi, and C.-X. Dong, Optical pumping through the liouvillian skin effect, *Phys. Rev. B* **111**, L060301 (2025).

[34] F. Song, S. Yao, and Z. Wang, Non-hermitian skin effect and chiral damping in open quantum systems, *Phys. Rev. Lett.* **123**, 170401 (2019).

[35] T. Mori and T. Shirai, Resolving a discrepancy between liouvillian gap and relaxation time in boundary-dissipated quantum many-body systems, *Phys. Rev. Lett.* **125**, 230604 (2020).

[36] A. McDonald, R. Hanai, and A. A. Clerk, Nonequilibrium stationary states of quantum non-hermitian lattice models, *Phys. Rev. B* **105**, 064302 (2022).

[37] G. Lee, A. McDonald, and A. Clerk, Anomalously large relaxation times in dissipative lattice models beyond the non-hermitian skin effect, *Phys. Rev. B* **108**, 064311 (2023).

[38] R. Belyansky, C. Weis, R. Hanai, P. B. Littlewood, and A. A. Clerk, Phase transitions in nonreciprocal driven-dissipative condensates, *Phys. Rev. Lett.* **135**, 123401 (2025).

[39] M. Moroder, O. Culhane, K. Zawadzki, and J. Goold, Thermodynamics of the quantum mpemba effect, *Phys. Rev. Lett.* **133**, 140404 (2024).

[40] S. Longhi, Quantum mpemba effect from non-normal dynamics, *Entropy* **27**, 581 (2025).

[41] T. Prosen, Third quantization: a general method to solve master equations for quadratic open fermi systems, *New Journal of Physics* **10**, 043026 (2008).

[42] T. Prosen, Spectral theorem for the lindblad equation for quadratic open fermionic systems, *Journal of Statistical Mechanics: Theory and Experiment* **2010**, P07020 (2010).

[43] M. van Caspel, S. E. Tapias Arze, and I. Pérez Castillo, Dynamical signatures of topological order in the driven-dissipative kitaev chain, *SciPost Physics* **6**, 026 (2019).

[44] A. McDonald and A. A. Clerk, Third quantization of open quantum systems: Dissipative symmetries and connections to phase-space and keldysh field-theory formulations, *Phys. Rev. Res.* **5**, 033107 (2023).

[45] C.-E. Bardyn, M. A. Baranov, C. V. Kraus, E. Rico, A. İmamoğlu, P. Zoller, and S. Diehl, Topology by dissipation, *New Journal of Physics* **15**, 085001 (2013).

[46] L. Mao, F. Yang, and H. Zhai, Symmetry-preserving quadratic lindbladian and dissipation driven topological transitions in gaussian states, *Reports on Progress in Physics* **87**, 070501 (2024).

[47] D. C. Brody, Biorthogonal quantum mechanics, *Journal of Physics A: Mathematical and Theoretical* **47**, 035305 (2013).

[48] J. Dajka, J. Luczka, and P. Hänggi, Distance between quantum states in the presence of initial qubit-environment correlations: A comparative study, *Phys. Rev. A* **84**, 032120 (2011).

[49] S. Kumar, Wishart and random density matrices: Analytical results for the mean-square hilbert-schmidt distance, *Phys. Rev. A* **102**, 012405 (2020).

[50] R. A. Bertlmann, K. Durstberger, B. C. Hiesmayr, and P. Krammer, Optimal entanglement witnesses for qubits and qutrits, *Phys. Rev. A* **72**, 052331 (2005).

[51] R. A. Bertlmann and P. Krammer, Geometric entanglement witnesses and bound entanglement, *Phys. Rev. A* **77**, 024303 (2008).

[52] V. c. v. Trávníček, K. Bartkiewicz, A. Černoch, and K. Lemr, Experimental measurement of the hilbert-schmidt distance between two-qubit states as a means for reducing the complexity of machine learning, *Phys. Rev. Lett.* **123**, 260501 (2019).

[53] T. Sugiyama, P. S. Turner, and M. Murao, Precision-guaranteed quantum tomography, *Phys. Rev. Lett.* **111**, 160406 (2013).

[54] H. Zhu and B.-G. Englert, Quantum state tomography with fully symmetric measurements and product measurements, *Phys. Rev. A* **84**, 022327 (2011).

[55] A. Chaduteau, D. K. K. Lee, and F. Schindler, Lindbladian versus postselected non-hermitian topology, *Phys. Rev. Lett.* **136**, 016603 (2026).

[56] S. Lieu, M. McGinley, and N. R. Cooper, Tenfold way for quadratic lindbladians, *Phys. Rev. Lett.* **124**, 040401 (2020).

[57] A. Metelmann and A. A. Clerk, Nonreciprocal photon transmission and amplification via reservoir engineering, *Phys. Rev. X* **5**, 021025 (2015).

[58] C. C. Wanjura, M. Brunelli, and A. Nunnenkamp, Topological framework for directional amplification in driven-dissipative cavity arrays, *Nature communications* **11**, 3149 (2020).

[59] D. Porras and S. Fernández-Lorenzo, Topological amplification in photonic lattices, *Phys. Rev. Lett.* **122**, 143901 (2019).

[60] N. Hatano and D. R. Nelson, Localization transitions in non-hermitian quantum mechanics, *Phys. Rev. Lett.* **77**, 570 (1996).

[61] N. Hatano and D. R. Nelson, Vortex pinning and non-hermitian quantum mechanics, *Phys. Rev. B* **56**, 8651 (1997).

[62] N. Hatano and D. R. Nelson, Non-hermitian delocalization and eigenfunctions, *Phys. Rev. B* **58**, 8384 (1998).

[63] S. Yao and Z. Wang, Edge states and topological invariants of non-hermitian systems, *Phys. Rev. Lett.* **121**, 086803 (2018).

[64] S. Longhi, Quantum pontus-mpemba effect enabled by the liouvillian skin effect, *arXiv preprint arXiv:2601.14083* (2026).